

## Diffusion of colloidal particles in model porous media

Luhui Ning,<sup>1,2,\*</sup> Peng Liu<sup>1,2,\*</sup>, Fangfu Ye,<sup>1,2,3,4</sup> Mingcheng Yang<sup>1,2,3,†</sup> and Ke Chen<sup>1,2,3,‡</sup>

<sup>1</sup>Beijing National Laboratory for Condensed Matter Physics and Laboratory of Soft Matter Physics, Institute of Physics, Chinese Academy of Sciences, Beijing 100190, China

<sup>2</sup>University of Chinese Academy of Sciences, Beijing 100049, China

<sup>3</sup>Songshan Lake Materials Laboratory, Dongguan, Guangdong 523808, China

<sup>4</sup>Wenzhou Institute, University of Chinese Academy of Sciences, Wenzhou, Zhejiang 325001, China



(Received 27 October 2020; accepted 22 January 2021; published 11 February 2021)

Using video microscopy and simulations, we study the long-time diffusion of colloidal tracers in a wide range of model porous media composed of frozen colloidal matrices with different structures. We found that the diffusion coefficient of a tracer can be quantitatively determined by the structures of porous media. In particular, a universal scaling relation exists between the dimensionless diffusion coefficient of the tracer and the structural entropy of the system. This universal scaling relation is an extension of the scaling law previously discovered for the diffusion of colloidal particles in fluctuating media.

DOI: [10.1103/PhysRevE.103.022608](https://doi.org/10.1103/PhysRevE.103.022608)

### I. INTRODUCTION

Diffusion in porous media is ubiquitous in nature and is of broad scientific and technological importance in fields ranging from drug delivery [1–6], water filtration [7–11], DNA separation [12–20], solar cell production [21–23], to oil and gas exploration and storage [24–27]. In porous media, the solid matrix impedes the free diffusion of microparticles or molecules confined inside. The diffusive transport of mass in porous media is then affected by the degree of confinement, the microscopic structures of the matrix, and the particle-matrix interactions. The details of these factors are not always experimentally obtainable and may vary greatly between systems. As a result, a quantitative general understanding of diffusion in porous media is still lacking despite numerous studies on this phenomenon in a wide range of scenarios [28–44].

On the other hand, diffusions in thermally fluctuating media are relatively well understood. For the dilute case, the diffusion of a colloidal particle in a Newtonian fluid can be accurately described by the Stokes-Einstein relations. In medium or higher concentrations and with more complex structures, diverse scaling laws between the diffusion coefficient of a tagged particle and the structural entropy of the fluctuating fluid have been proposed [45–58] and experimentally tested [59–63]. More recently, Ning *et al.* [64] proposed and validated a universal scaling relation in colloidal systems with a wider range of fluctuating media including both disordered and ordered structures. The normalized diffusion coefficient  $D^*$  of the tracer is related to the two-body

structural entropy  $S_2$  by

$$D^* = \frac{k_B T}{\Gamma d_s^2 \xi_B} \frac{1}{A(1 - S_2) + \xi_S / \xi_B}, \quad (1)$$

with  $k_B T$  as the thermal energy,  $\Gamma$  as the Enskog collision frequency,  $d_s$  as the tracer diameter,  $\xi_B$  as the Enskog binary collision friction,  $\xi_S$  as the Stokes friction from the solvent, and  $A$  as the only fitting parameter. When  $\xi_S = 0$ , Eq. (1) reduces to the scaling relation for molecular systems [51]. This universal scaling relation identifies the key factors affecting the diffusion dynamics in complex environments and is generally applicable in a wide range of fluctuating media. Additionally, an amount of work has been devoted to examining the validity of the diffusion scaling law in fluids confined under regular geometry [65–72]. However, the corresponding experimental study is quite rare, mainly due to the difficulty in measuring the structural entropy in such systems.

With the success of the universal scaling law for diffusion in thermally fluctuating environment, an interesting question is whether similar universal relation exists for porous media whose structures are frozen. A straightforward generalization of the scaling relation from fluctuating environment to porous media is not obvious as the porous media differ from the fluctuating environment in several important aspects. First, the microscopic collision kinetics between the tracer and the media elements are fundamentally different for the immobile porous media and fluctuating backgrounds. Second, both static and dynamical structures of the frozen and fluctuating media are different. The structures of frozen media are fixed with inhomogeneities that do not relax over time, whereas the structures of thermally fluctuating media are in thermal equilibrium, thus, more homogeneous. Structural heterogeneity and the absence of structural relaxation in frozen media may lead to more heterogeneous diffusion patterns for the tracer particles. For example, in the frozen media a gap smaller than the particles size permanently forbids a particle from

\*These authors contributed equally to this work.

†mcyang@iphy.ac.cn

‡kechen@iphy.ac.cn

passing through, whereas in fluctuating media, there exist a nontrivial probability that thermal fluctuations may widen the gap to allow such diffusion path to take place. Third, it is difficult to determine the structural entropy in the porous media. Structural entropy is derived from the spatial correlations in pointlike systems, whereas many real porous media consist of irregular building blocks with complex connections that cannot be easily treated as point patterns. Therefore, it is not immediately clear that the diffusion scaling law in thermally fluctuating media is directly applicable in frozen porous environments.

In this paper, by means of experiments and simulations, we systematically study the diffusion coefficients of colloidal tracers in model porous media formed by immobile colloidal particles. Both experiments and simulations are performed in hexagonal and disordered backgrounds with additional simulations in quasicrystalline and square lattices. We simultaneously measure the tracer diffusion coefficient and the two-body structure entropy of the system with different structures and densities. Remarkably, we find that the tracer diffusion coefficients can still be quantitatively related to the two-body structure entropy through the scaling relation of Eq. (1) with a minimal modification by considering the mass of the frozen constituent element to be infinite. This finding establishes the diffusion-structure relation in porous media that can be quantitatively applied to diffusions in a wide range of situations.

## II. EXPERIMENTS AND SIMULATIONS

The experiments are performed in a quasi-two-dimensional (2D) configuration using a bidisperse aqueous solution of polystyrene (PS) particles hermetically sealed between two coverslips. The porous background is modeled by a matrix of large polystyrene particles (diameter  $d_l = 1.0 \mu\text{m}$ ) fixed in regions where the separation between the coverslips is less than the effective diameter of the large PS spheres. The structure of the background is thus frozen with no structural relaxations during the experiments. The ordered matrices are formed by shearing the colloidal suspension during the sample preparation and later rendered immobile by the confining glass walls. The small colloidal particles (diameters  $d_s = 0.35$  or  $0.56 \mu\text{m}$ ), on the other hand, are allowed to diffuse in these regions as the wall separation is significantly greater than the particle diameter [73,74]. The large PS particles that form the background are strongly negatively charged by sulfonation [75]; the strong repulsion between these particles creates interparticle gaps wide enough for the small particles to diffuse through. To minimize the correlations between the diffusing tracers, the number density of the small particles is kept low with the average tracer density  $\sim 0.0015 \mu\text{m}^{-2}$ . The images of the samples are acquired using bright field video microscopy with an oil-immersed  $\times 100$  objective at 55 fps. During the experiments, the focal plane is kept near the center of the large PS spheres, and the tracer particles fluctuate near the focal plane due to their smaller sizes. Figure 1 shows the snapshots in experiments with different porous matrices. The positions of the particles are extracted using particle tracking techniques [76]. The frozen matrix particles and the diffusing tracers are differentiated based on their integrated brightness.

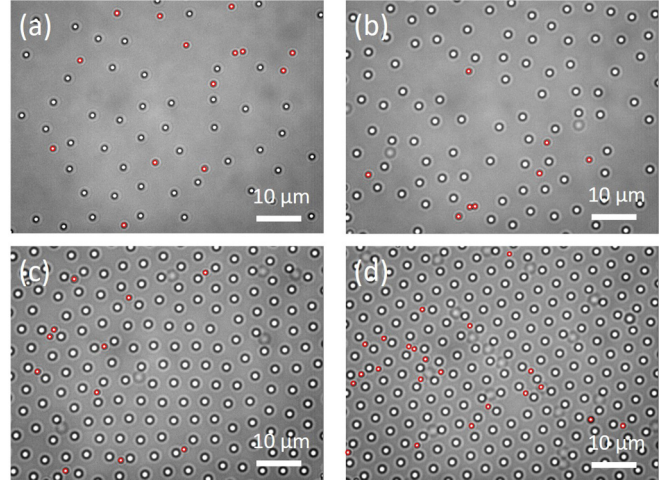


FIG. 1. Snapshots of tracer particles diffusing in frozen matrices with (a)–(c) disordered structures and (d) a crystalline structure, formed by large strongly charged PS particles. The large bright particles are the frozen PS particles, and the small ones marked by red circles are the free tracer particles.

In simulations, the porous media consists of 1600 large particles frozen in a 2D box with periodic boundary conditions. We consider four different structures of frozen matrices, including a disordered structure, a square lattice, a hexagonal lattice, and a quasicrystal in which the small tracer particle diffuses as sketched in Fig. 2. The diameter of the tracer particle  $d_s$  is 1/4 of that of the fixed matrix particle  $d_l = 2.0$ . The interaction between the tracer and the frozen matrix particles is described by the repulsive Lennard-Jones type potential  $U(r) = 4\epsilon[(\frac{\sigma}{r})^{2n} - (\frac{\sigma}{r})^n] + \epsilon$ ,  $r < 2^{1/n}\sigma$  with the interaction intensity  $\epsilon = 1.0$  equal to the thermal energy  $k_B T$  and the interaction diameter  $\sigma = (d_l + d_s)/2$ . In simulations,

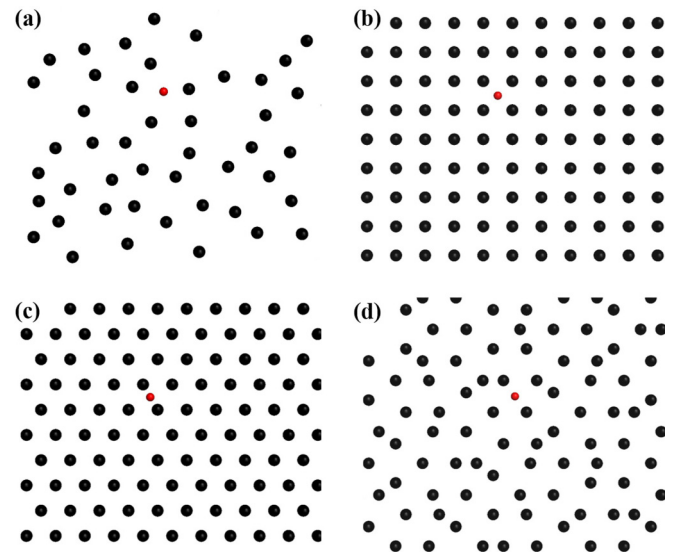


FIG. 2. Schematics of the tracer particle diffusing in (a) the disordered, (b) the square lattice, (c) the hexagonal lattice, and (d) the quasi-crystal solid matrices. The large black and small red circles represent the frozen particles of the porous media and the tracer particle, respectively.

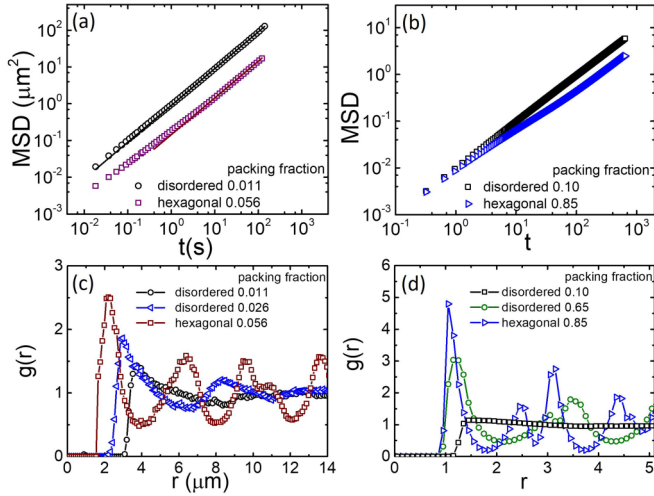


FIG. 3. The MSDs of the small tracer particles in (a) experiments and in (b) simulations, and the  $g(r)$  of the large matrix particles with respect to the free tracer in experiments (c) and in simulations (d) in different porous media. The solid lines in (a) are the best fit to  $\langle \Delta \mathbf{r}^2(t) \rangle = 4Dt$  at long times. The numbers in the legend refer to the packing fractions of the large matrix particles.

the potential stiffness  $n = 2$  and  $n = 6$  are both employed to verify the robustness of the simulation results, and the packing fraction of the large frozen particles varies widely to achieve a large range of structural entropy. The dynamics of the tracer particle in the frozen porous media is described by the overdamped Langevin equation,

$$\gamma \dot{\mathbf{r}} = -\nabla U(r) + \boldsymbol{\eta}. \quad (2)$$

Here,  $\gamma$  is the translational friction coefficient of the probe particle, and  $\boldsymbol{\eta}$  refers to the Gaussian distributed stochastic force with  $\langle \boldsymbol{\eta}(t) \rangle = 0$  and  $\langle \eta_\alpha(t) \eta_\beta(t') \rangle = 2k_B T \gamma \delta_{\alpha\beta} \delta(t - t')$ . The equation of motion is integrated with the time step  $\Delta t = 10^{-3} \sqrt{m_s d_l^2 / \epsilon}$ . Here,  $m_s = 1$  represents the mass of the tracer particle.

### III. RESULTS AND DISCUSSIONS

#### A. Tracer dynamics and structural entropy

In both experiments and simulations, the tracer dynamics are characterized by the long-time diffusion coefficient  $D$ , extracted from the mean square displacements (MSDs)  $\langle \Delta \mathbf{r}^2(t) \rangle = \langle [\mathbf{r}(t_0 + t) - \mathbf{r}(t_0)]^2 \rangle$  of the tracers at long times where the  $\langle \dots \rangle$  represents the ensemble average. Figure 3(a) shows the log-log plot of the MSDs of the probe particles as a function of delay time  $t$  in the fixed media in experiments at two different packing fractions 0.011 and 0.056. The packing fractions are calculated from the hydrodynamic diameter and number density of the background particles. The long-time diffusion coefficient  $D$  is obtained by linearly fitting the MSD curves at long times with  $\langle \Delta \mathbf{r}^2(t) \rangle = 4Dt$ . Typical tracer MSDs from simulations are plotted in Fig. 3(b) at slightly higher packing fractions of the matrix particles than those in the experiments. The long-time diffusion coefficient in simulations is obtained in the same way as in the experiments.

The structure of the system is characterized by the structural entropy of the system. The structural entropy, which is also known as the excess entropy, is the entropy difference between a many-body system and the ideal gas under equivalent conditions due to structural correlations. In principle, all positional correlations (including two-body, three-body, four-body... $(N - 1)$ -body correlations) should be taken into account when evaluating the structural entropy. In practice, however, two-body correlation, thus,  $S_2$  contributes more than 85% of the total structural entropy in a wide range of density [77], which is employed in our experiments and simulations. Thus, the structural entropy for the tracer in the matrix can be obtained from the measured pair correlations function  $g(r)$  of the matrix particles with respect to the diffusing tracer, using the following formula:

$$S_2 = -\pi \rho \int_0^\infty \{g(r) \ln[g(r)] - [g(r) - 1]\} r dr, \quad (3)$$

as in the fluctuating environment [59–61,64]. Here,  $\rho$  is the mean number density of the background particles. The pair correlation function  $g(r)$  is the relative probability of finding another particle at the distance  $r$  from a reference particle [78,79], and  $g(r)$  measured from the perspective of the tracer particles can be expressed as

$$g(r) = \frac{1}{2\pi r \rho} \left\langle \frac{1}{N_s} \sum_i \sum_j \delta(r - r_{ij}) \right\rangle. \quad (4)$$

Here,  $N_s$  and  $N_l$  represent the total number of tracer particles and background large particles, respectively, and  $r_{ij}$  is the distance between the tracer particle  $i$  and the background particle  $j$ .

Figure 3(c) plots  $g(r)$  at different packing fractions of the frozen matrix in experiments. As the packing fraction increases, the position of the first peak of  $g(r)$  shifts to lower values. And at the highest density,  $g(r)$  exhibits periodic features as the background media become crystalline.  $g(r)$  measured in different background structures in simulations are plotted in Fig. 3(d). In the experiments,  $S_2$  decreases with the particle density for disordered backgrounds. And in the crystalline backgrounds,  $S_2$  depends primarily on the lattice quality as the lattice constant varies over a small range. In the simulations, the lattices constant of crystalline media are systematically varied, the  $S_2$  increases with the lattice spacing due to the lower particle density at larger lattice constants.

#### B. Correlations between diffusion dynamics and structural entropy

To compare the tracer diffusion coefficients measured in different backgrounds, we follow previous works to normalize the diffusion coefficients by  $D^* = D \Gamma^{-1} d_s^{-2}$ , rendering them dimensionless [64]. Here,  $\Gamma$  is the Enskog collision frequency between the tracer and the frozen large particles in the 2D system and is calculated by [61,64]

$$\Gamma = 2\sigma \rho g(\sigma) \sqrt{\pi k_B T / m}, \quad (5)$$

where  $\sigma$  refers to the position of the first peak of  $g(r)$  and  $m = 2m_s m_l / (m_s + m_l)$  is the reduced mass of the tracer particle with  $m_s$  and  $m_l$  separately representing the masses of the

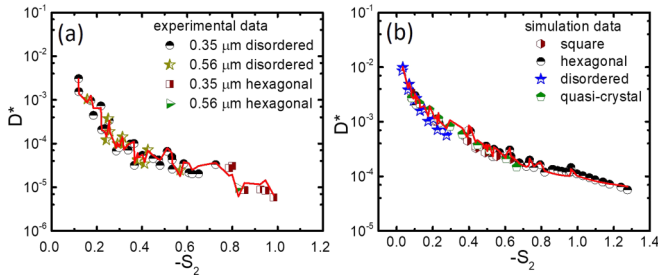


FIG. 4. The dimensionless diffusion coefficient  $D^*$  of the tracers as a function of the two-body structural entropy in porous media. The symbols in (a) are the measured  $D^*$  in experiments with different combinations of tracer sizes and matrix structures. The symbols in (b) represent the measured  $D^*$  in four different matrix structures in simulations, including the disordered, the square lattice, the hexagonal lattice, and the quasicrystalline lattice. The red solid lines represent the fit to the data using Eq. (1) with  $\Gamma$ ,  $\xi_B$ , and  $\xi_S$  obtained from independent calculations.

tracer and the fixed background particle. As the background particles are fixed, they can be considered as part of a rigid body which includes all the background particles and the glass slides. Therefore, the collision between the tracer particle and the fixed background particle can be well approximated by collisions between the tracer and a rigid body with infinite mass. By taking the mass of the matrix particles in the frozen background to be  $m_l = \infty$ , the reduced mass for collisions becomes  $m = 2m_s$ .

Figure 4(a) plots the normalized diffusion coefficients  $D^*$  of tracers of two different sizes as functions of  $S_2$  in ordered and disordered backgrounds in experiments. All the data from frozen media collapse onto a single master curve as in the case of the fluctuating environments [64], which clearly suggests that there exists a universal relation between the diffusion dynamics and the structural entropy in the porous media, insensitive to the specific tracer type or the structural details of the media. Remarkably, a good quantitative agreement is reached between the experimental data and the theory when Eq. (1) is applied to the measured  $D^*$  and  $S_2$  in Fig. 4(a). The red solid line is the theoretically predicted dimensionless diffusion coefficient as a function of  $S_2$ , which overlaps with experimental data over several decades of  $D^*$ . This universal scaling relation is further confirmed by simulations with more matrix structures, including disordered, hexagonal lattice, square lattice, and quasicrystalline structures. Figure 4(b) plots the dimensionless diffusion coefficient as a function of  $S_2$  in different matrices in simulations. Similar to experiments, all simulation data collapse to a master curve, and quantitative agreement with Eq. (1) is observed over several orders of magnitude. We note that when comparing the experimental

or simulation results to Eq. (1), the  $\Gamma$  and  $\xi_B$  are evaluated by setting the mass of the frozen background particles to infinity. The good agreement between the theory and the measured diffusion coefficients suggests that this assumption is practically reasonable for the model porous media. These results unambiguously show that the tracer diffusion coefficient in porous media is determined by the structural entropy, and the dynamics-structure relation is essentially the same in both thermally fluctuating media and frozen porous media with a small modification to the mass of the media elements.

We note that the normalized diffusion coefficients measured in the frozen media are significantly lower than those observed in fluctuating media as reported in Ref. [64]. These differences may be attributed to the composition of the two systems, including the tracer sizes and the chemical properties of the particles. The tracer dynamics is further slowed down in the frozen media from the lack of structural relaxations of the background, which limits the number of available paths of diffusion.

#### IV. CONCLUSIONS

To summarize, we study the long-time diffusion dynamics of tracer particles in model porous media composed of frozen colloidal particles in 2D, using microscopy experiments and computer simulations. The normalized diffusion coefficient of the tracers is uniquely determined by the structural entropy of the system for a wide range of structure and density of the porous media, thus, establishing a universal scaling relation between diffusion dynamics and system structure. This universal scaling law is reminiscent of the previously discovered scaling relation in fluctuating colloidal matrices, despite the qualitative differences between the two types of media. In particular, the functional forms of the two scaling relations become identical when the mass of the particles in the frozen matrix is set to infinity. Thus, the present paper significantly extends the universal relation between diffusing dynamics and system structures from thermal media to frozen media and allows quantitative prediction, control, and design of diffusions in frozen media. Our finding constitutes an important step towards a general and quantitative diffusion-structure relation in real porous media where the determination of system structural entropy beyond pointlike patterns remains an open question.

#### ACKNOWLEDGMENTS

We thank R. Liu for helpful discussions, and we acknowledge support from the National Natural Science Foundation of China (Grants No. 11874395, No. 11874397, No. 11674365, No. 11474327, and No. 12047552). This work was also supported by the Strategic Priority Research Program of Chinese Academy of Sciences (Grant No. XDB33000000).

- [1] H. S. El-Sawy, A. M. Al-Abd, T. A. Ahmed, K. M. El-Say, and V. P. Torchilin, *ACS Nano* **12**, 10636 (2018).  
 [2] G. Jeon, S. Y. Yang, J. Byun, and J. K. Kim, *Nano Lett.* **11**, 1284 (2011).

- [3] T. Lebold, C. Jung, J. Michaelis, and C. Bräuchle, *Nano Lett.* **9**, 2877 (2009).  
 [4] W. Li, Z. Liu, F. Fontana, Y. Ding, D. Liu, J. T. Hirvonen, and H. A. Santos, *Adv. Mater.* **30**, e1703740 (2018).

- [5] E. N. Abramova, A. M. Khort, A. G. Yakovenko, D. S. Kornilova, E. A. Slipchenko, D. I. Prokhorov, and V. I. Shvets, *J. Phys.: Conf. Ser.* **945**, 012001 (2018).
- [6] H. Zhang, D. Liu, M.-A. Shahbazi, E. Mäkilä, B. Herranz-Blanco, J. Salonen, J. Hirvonen, and H. A. Santos, *Adv. Mater.* **26**, 4497 (2014).
- [7] E. A. Jackson and M. A. Hillmyer, *ACS Nano* **4**, 3548 (2010).
- [8] D. S. Goldobin and B. S. Maryshev, *J. Phys.: Conf. Ser.* **894**, 012062 (2017).
- [9] M. Liang, C. Fu, B. Xiao, L. Luo, and Z. Wang, *Int. J. Heat Mass Transf.* **137**, 365 (2019).
- [10] A. Revil, *Adv. Water Resour.* **103**, 139 (2017).
- [11] Y. Davit, H. Byrne, J. Osborne, J. Pitt-Francis, D. Gavaghan, and M. Quintard, *Phys. Rev. E* **87**, 012718 (2013).
- [12] J. Han and H. G. Craighead, *Science* **288**, 1026 (2000).
- [13] Z. Cao, Y. Zhu, Y. Liu, S. Dong, J. Zhao, Y. Wang, S. Yang, and J. Fu, *Biosens. Bioelectron.* **137**, 8 (2019).
- [14] P. S. Doyle, J. Bibette, A. Bancaud, and J.-L. Viovy, *Science* **295**, 2237 (2002).
- [15] S. W. P. Turner, M. Cabodi, and H. G. Craighead, *Phys. Rev. Lett.* **88**, 128103 (2002).
- [16] M. Baba, T. Sano, N. Iguchi, K. Iida, T. Sakamoto, and H. Kawaura, *Appl. Phys. Lett.* **83**, 1468 (2003).
- [17] J. Fu, R. B. Schoch, A. L. Stevens, S. R. Tannenbaum, and J. Han, *Nat. Nanotechnol.* **2**, 121 (2007).
- [18] T. Yasui, N. Kaji, R. Ogawa, S. Hashioka, M. Tokeshi, Y. Horiike, and Y. Baba, *Anal. Chem.* **83**, 6635 (2011).
- [19] T. Yasui, S. Rahong, K. Motoyama, T. Yanagida, Q. Wu, N. Kaji, M. Kanai, K. Doi, K. Nagashima, M. Tokeshi *et al.*, *ACS Nano* **7**, 3029 (2013).
- [20] S. Rahong, T. Yasui, T. Yanagida, K. Nagashima, M. Kanai, G. Meng, Y. He, F. Zhuge, N. Kaji, T. Kawai *et al.*, *Anal. Sci.* **31**, 153 (2015).
- [21] Z. Shao and S. M. Haile, *Nature (London)* **431**, 170 (2004).
- [22] S. J. Harris, A. Timmons, D. R. Baker, and C. Monroe, *Chem. Phys. Lett.* **485**, 265 (2010).
- [23] S. Khurana, S. Johnson, A. Karimghaloo, and M. H. Lee, *Int. J. Precision Eng. Manufacturing-Green Technol.* **5**, 637 (2018).
- [24] J. Xu, L. Jianming, W. Xiaoqi, L. He, and L. Xiaodan, *Energy Procedia* **158**, 5962 (2019).
- [25] R. Ponnappati, O. Karazincir, E. Dao, R. Ng, K. K. Mohanty, and R. Krishnamoorti, *Ind. Eng. Chem. Res.* **50**, 13030 (2011).
- [26] D. P. Broom, C. J. Webb, K. E. Hurst, P. A. Parilla, T. Gennett, C. M. Brown, R. Zacharia, E. Tylisanakis, E. Klontzas, G. E. Froudakis *et al.*, *Appl. Phys. A: Mater. Sci. Process.* **122**, 151 (2016).
- [27] S. Rochat, K. Polak-Kraśna, M. Tian, L. T. Holyfield, T. J. Mays, C. R. Bowen, and A. D. Burrows, *J. Mater. Chem. A* **5**, 18752 (2017).
- [28] W. D. Volkmuth and R. H. Austin, *Nature (London)* **358**, 600 (1992).
- [29] D. Nykypanchuk, H. H. Strey, and D. A. Hoagland, *Science* **297**, 987 (2002).
- [30] Y. Su, P.-Y. Lai, B. J. Ackerson, X. Cao, Y. Han, and P. Tong, *J. Chem. Phys.* **146**, 214903 (2017).
- [31] D. M. Tartakovsky and M. Dentz, *Transp. Porous Media* **130**, 105 (2019).
- [32] N. Ray, A. Rupp, R. Schulz, and P. Knabner, *Transp. Porous Media* **124**, 803 (2018).
- [33] R. Raccis, A. Nikoubashman, M. Retsch, U. Jonas, K. Koynov, H.-J. Butt, C. N. Likos, and G. Fytas, *ACS Nano* **5**, 4607 (2011).
- [34] K. He, F. B. Khorasani, S. T. Retterer, D. K. Thomas, J. C. Conrad, and R. Krishnamoorti, *ACS Nano* **7**, 5122 (2013).
- [35] T. O. E. Skinner, S. K. Schnyder, D. G. A. L. Aarts, J. Horbach, and R. P. A. Dullens, *Phys. Rev. Lett.* **111**, 128301 (2013).
- [36] D. Wang, C. He, M. P. Stoykovich, and D. K. Schwartz, *ACS Nano* **9**, 1656 (2015).
- [37] M. J. Skaug, L. Wang, Y. Ding, and D. K. Schwartz, *ACS Nano* **9**, 2148 (2015).
- [38] S. Amitai and R. Blumenfeld, *Granular Matter* **19**, 13 (2017).
- [39] G. Viramontes-Gamboa, J. L. Arauz-Lara, and M. Medina-Noyola, *Phys. Rev. Lett.* **75**, 759 (1995).
- [40] J. Kurzidim, D. Coslovich, and G. Kahl, *Phys. Rev. Lett.* **103**, 138303 (2009).
- [41] C. Giraudet, M. S. G. Knoll, Y. Galvan, S. Süß, D. Segets, N. Vogel, M. H. Rausch, and A. P. Fröba, *Transp. Porous Media* **131**, 723 (2020).
- [42] Y. Ye, Z. Du, M. Tian, L. Zhang, and J. Mi, *Phys. Chem. Chem. Phys.* **19**, 380 (2017).
- [43] F. Liu, S. M. Abel, L. Collins, B. R. Srijanto, R. Standaert, J. Katsaras, and C. P. Collier, *Adv. Mater. Interfaces* **6**, 1900054 (2019).
- [44] D. Wang, H. Wu, L. Liu, J. Chen, and D. K. Schwartz, *Phys. Rev. Lett.* **123**, 118002 (2019).
- [45] M. Dzugutov, *Nature (London)* **381**, 137 (1996).
- [46] Y. Rosenfeld, *J. Phys.: Condens. Matter* **11**, 5415 (1999).
- [47] J. J. Hoyt, M. Asta, and B. Sadigh, *Phys. Rev. Lett.* **85**, 594 (2000).
- [48] A. Samanta, S. M. Ali, and S. K. Ghosh, *Phys. Rev. Lett.* **87**, 245901 (2001).
- [49] J.-L. Bretonnet, *J. Chem. Phys.* **117**, 9370 (2002).
- [50] S. Bastea, *Phys. Rev. E* **68**, 031204 (2003).
- [51] A. Samanta, S. M. Ali, and S. K. Ghosh, *Phys. Rev. Lett.* **92**, 145901 (2004).
- [52] J. L. Bretonnet, *J. Chem. Phys.* **120**, 11100 (2004).
- [53] C. Kaur, U. Harbola, and S. P. Das, *J. Chem. Phys.* **123**, 034501 (2005).
- [54] G. X. Li, C. S. Liu, and Z. G. Zhu, *Phys. Rev. B* **71**, 094209 (2005).
- [55] S. N. Chakraborty and C. Chakravarty, *J. Chem. Phys.* **124**, 014507 (2006).
- [56] M. Malvaldi and C. Chiappe, *J. Chem. Phys.* **132**, 244502 (2010).
- [57] M. Agarwal, M. Singh, B. S. Jabes, and C. Chakravarty, *J. Chem. Phys.* **134**, 014502 (2011).
- [58] J. C. Dyre, *J. Chem. Phys.* **149**, 210901 (2018).
- [59] X. Ma, W. Chen, Z. Wang, Y. Peng, Y. Han, and P. Tong, *Phys. Rev. Lett.* **110**, 078302 (2013).
- [60] A. L. Thorneywork, R. E. Rozas, R. P. A. Dullens, and J. Horbach, *Phys. Rev. Lett.* **115**, 268301 (2015).
- [61] C.-H. Wang, S.-H. Yu, and P. Chen, *Phys. Rev. E* **91**, 060201(R) (2015).
- [62] X. Ma, J. Liu, Y. Zhang, P. Habdas, and A. G. Yodh, *J. Chem. Phys.* **150**, 144907 (2019).
- [63] K. L. Galloway, X. Ma, N. C. Keim, D. J. Jerolmack, A. G. Yodh, and P. E. Arratia, *Proc. Natl. Acad. Sci. USA* **117**, 11887 (2020).
- [64] L. Ning, P. Liu, Y. Zong, R. Liu, M. Yang, and K. Chen, *Phys. Rev. Lett.* **122**, 178002 (2019).

- [65] B. J. Borah, P. K. Maiti, C. Chakravarty, and S. Yashonath, *J. Chem. Phys.* **136**, 174510 (2012).
- [66] P. He, H. Li, and X. Hou, *Chem. Phys. Lett.* **593**, 83 (2014).
- [67] Y. Liu, J. Fu, and J. Wu, *Langmuir* **29**, 12997 (2013).
- [68] P. He, H. Liu, J. Zhu, Y. Li, S. Huang, P. Wang, and H. Tian, *Chem. Phys. Lett.* **535**, 84 (2012).
- [69] J. Mittal, J. R. Errington, and T. M. Truskett, *Phys. Rev. Lett.* **96**, 177804 (2006).
- [70] J. Mittal, J. R. Errington, and T. M. Truskett, *J. Phys. Chem. B* **111**, 10054 (2007).
- [71] R. Chopra, T. M. Truskett, and J. R. Errington, *Phys. Rev. E* **82**, 041201 (2010).
- [72] M. Zarif and R. K. Bowles, *Phys. Rev. E* **101**, 012908 (2020).
- [73] G. Cruz de León, J. M. Saucedo-Solorio, and J. L. Arauz-Lara, *Phys. Rev. Lett.* **81**, 1122 (1998).
- [74] G. Cruz de León and J. L. Arauz-Lara, *Phys. Rev. E* **59**, 4203 (1999).
- [75] M. Hazarika, K. Malkappa, and T. Jana, *Polym. Int.* **61**, 1425 (2012).
- [76] J. C. Crocker and D. G. Grier, *J. Colloid Interface Sci.* **179**, 298 (1996).
- [77] A. Baranyai and D. J. Evans, *Phys. Rev. A* **40**, 3817 (1989).
- [78] J.-P. Hansen and I. R. McDonald, *Theory of Simple Liquids: With Applications to Soft Matter* (Academic Press, Amsterdam, 2013).
- [79] A. L. Thorneywork, R. Roth, D. G. A. L. Aarts, and R. P. A. Dullens, *J. Chem. Phys.* **140**, 161106 (2014).